Earth Syst. Dynam. Discuss., doi:10.5194/esd-2015-88, 2016
Manuscript under review for journal Earth Syst. Dynam.
Published: 18 January 2016

Earth System Dynamics
Discussions
Open Access

Vegetation-climate feedbacks modulate rainfall patterns in Africa under future climate change

M. Wu[1], G. Schurgers[2], M. Rummukainen[1,3], B. Smith[1], P. Samuelsson[4], C. Jansson[4], J. Siltberg[1], W. May[3]

[1]{Department of Physical Geography and Ecosystem Science, Lund University, Sölvegatan 12, SE-223 62, Lund, Sweden}

[2]{Department of Geosciences and Natural Resource Management, University of Copenhagen, Øster Voldgade 10, DK-1350 Copenhagen, Denmark}

[3]{Centre for Environmental and Climate Research, Lund University, Sölvegatan 37, SE-223 62 Lund, Sweden}

[4]{Rossby Centre, Swedish Meteorological and Hydrological Institute, SE-601 76, Norrköping, Sweden}

Correspondence to: M. Wu (minchao.wu@nateko.lu.se)

Earth Syst. Dynam. Discuss., doi:10.5194/esd-2015-88, 2016
Manuscript under review for journal Earth Syst. Dynam.
Published: 18 January 2016

Abstract

Africa has been undergoing significant changes in climate patterns and vegetation in recent decades, and continued changes may be expected over this century. Vegetation cover and composition impose important influences on the regional climate in Africa. Climate change-driven changes in regional vegetation patterns may feed back to climate via shifts in surface energy balance, hydrological cycle and resultant effects on surface pressure patterns and larger-scale atmospheric circulation. We used a regional Earth system model incorporating interactive vegetation-atmosphere coupling to investigate the potential role of vegetation-mediated biophysical feedbacks on climate dynamics in Africa in an RCP8.5-based future climate scenario. The model was applied at high resolution (0.44 x 0.44 degrees) for the CORDEX-Africa domain with boundary conditions from the CanESM2 GCM. We found that changes in vegetation patterns associated with a CO_2 and climate-driven increase in net primary productivity, particularly over sub-tropical savannah areas, not only imposed important local effect on the regional climate by altering surface energy fluxes, but also resulted in remote effects over central Africa by modulating the land-ocean temperature contrast, Atlantic Walker circulation and moisture inflow feeding the central African tropical rainforest region with precipitation. The vegetation-mediated feedbacks were in general negative with respect to temperature, dampening the warming trend simulated in the absence of feedbacks, and positive with respect to precipitation, enhancing rainfall reduction over rainforest areas. Our results highlight the importance of vegetation-atmosphere interactions in climate projections for tropical and sub-tropical Africa.

Keywords: RCA-GUESS, Vegetation feedback, Precipitation, Walker Circulation, land-ocean contrast

Earth Syst. Dynam. Discuss., doi:10.5194/esd-2015-88, 2016
Manuscript under review for journal Earth Syst. Dynam.
Published: 18 January 2016

Earth System Dynamics
Discussions
Open Access

1. Introduction

The Sahel greening and Congo rainforest browning observed since the 1980s suggest that Africa has been undergoing significant vegetation changes in structure and composition during the recent decades (Zhou et al., 2014;Eklundh and Olsson, 2003;Olsson et al., 2005;Jamali et al., 2014). In addition to influences from anthropogenic activity (e.g. changes in land use), vegetation shifts in the region have been linked to changes in recorded climatic conditions including the trend and interannual variability of precipitation (Herrmann et al., 2005;Olsson et al., 2005;Zhou et al., 2014;Hickler et al., 2005), which in turn have been related to decadal-scale changes in regional circulation (Camberlin et al., 2001;Giannini et al., 2003).

Shifts in vegetation composition, cover and seasonality (phenology) can in turn impose significant feedbacks on the physical climate system by altering surface-atmosphere energy exchange and hydrological cycling (biophysical feedbacks) as well as greenhouse gas concentrations and aerosol loads in the atmosphere (biogeochemical feedbacks). The type and coverage of vegetation are important to surface albedo, roughness length and evapotranspiration, affecting surface energy fluxes that in turn control lower boundary layer thermodynamics (Bonan, 2008;Brovkin et al., 2006;Eltahir, 1996). Biophysical feedbacks operate locally and may also generate teleconnections via heat and moisture advection, leading to altered circulation patterns (e.g. Avissar and Werth, 2005;Nogherotto et al., 2013).

There is an increasing awareness of the significance of biophysical vegetation-climate interaction for Africa. Vegetation changes in the Sahel can alter local decadal-scale precipitation variability through changes in local energy and water fluxes and even through changes in atmospheric circulation (Charney, 1975;Xue and Shukla, 1996;Wang and Eltahir,

Earth Syst. Dynam. Discuss., doi:10.5194/esd-2015-88, 2016
Manuscript under review for journal Earth Syst. Dynam.
Published: 18 January 2016

2000), while deforestation in the Congo basin increases surface albedo and weakens local moisture convection, resulting in decreased precipitation (Eltahir, 1996;Xue and Shukla, 1993;Bell et al., 2015;Nogherotto et al., 2013).

Anthropogenic climate change may lead to profound structural and compositional changes in the natural vegetation over Africa, especially for savannah areas where seasonal fluctuations in water availability and climate-mediated disturbance regimes (fires and grazing) serve to facilitate coexistence of trees and grasses in a fine competitive balance (Moncrieff et al., 2014;Sankaran et al., 2005;Doherty et al., 2010;Ahlström et al., 2015). Changed vegetation patterns may be expected to modulate the regional climate development. However, high-resolution studies of future vegetation-atmosphere coupling have not been performed earlier for Africa with a comprehensive approach.

We employ a regional Earth system model (ESM) that couples the physical component of a regional climate model (RCM) with a detailed, individual-based dynamic vegetation model (DVM). This tool enables dynamic representation of biophysical interactions between the vegetated land surface and the atmosphere and their effects on the evolution of climate and land surface biophysical properties to be analysed in an explicit way. We perform simulations under Representative Concentration Pathway (RCP) 8.5 future radiative forcing (Moss et al., 2010) with and without vegetation feedbacks enabled, and investigate the potential coupled evolution of climate and vegetation patterns for the CORDEX-Africa domain over the 21st century. Our focus is especially on the central African rainforest areas and the surrounding savannah vegetation belt.

2. Data and Method

2.1 Model description

Earth Syst. Dynam. Discuss., doi:10.5194/esd-2015-88, 2016
Manuscript under review for journal Earth Syst. Dynam.
Published: 18 January 2016

RCA-GUESS (Smith et al., 2011) is a regional ESM based on the Rossby Centre regional climate model RCA4 (Kjellström et al., 2005;Samuelsson et al., 2011) coupled with vegetation dynamics from the LPJ-GUESS DVM to account for land-atmosphere biophysical coupling (Smith et al., 2001;Smith et al., 2014).

The RCA4-based physical component of the model incorporates advanced regional surface heterogeneity, such as complex topography and multi-level presentations for forests and lakes, which are significant in controlling the development of weather events from the local- to meso-scale (Samuelsson et al., 2011). RCA4 has been successfully applied in a range of climate studies worldwide (e.g., Sörensson and Menéndez, 2011;Kjellström et al., 2011;Döscher et al., 2010). The land surface scheme (LSS, Samuelsson et al., 2006) adopts a tile approach and characterizes land surface with open land and forest tiles with separated energy balance. The open land tile is divided into fractions for vegetation (herbaceous vegetation) and bare soil. The forest tile is vertically divided into three sub-levels (canopy, forest floor and soil). Snow can exist in open land and/or forest tile as fractional cover. Surface properties such as surface temperature, humidity and turbulent heat fluxes (latent and sensible heat fluxes) for different tiles in a grid box are weighted together to provide grid-averaged surface boundary conditions. A detailed description is given by Samuelsson et al. (2006).

The vegetation dynamics component of RCA-GUESS employs a plant individual and patch-based representation of the vegetated landscape, optimized for studies at regional and global scale. Heterogeneities of vegetation structure and their effects on ecosystem functions such as carbon and water vapour exchange with the atmosphere are represented dynamically, affected by allometric growth of age-size classes of woody plant individuals,

Earth Syst. Dynam. Discuss., doi:10.5194/esd-2015-88, 2016
Manuscript under review for journal Earth Syst. Dynam.
Published: 18 January 2016

along with a grass understorey, and their interactions in competition for limited light and soil resources. Plant functional types (PFTs) encapsulate the differential functional responses of potentially-occurring species in terms of growth form, bioclimatic distribution, phenology, physiology and life-history characteristics. Multiple patches in each vegetated tile account for the effects of stochastic disturbances, establishment and mortality on local stand history (Smith et al., 2001). This explicit, dynamic representation of vertical structure and landscape heterogeneity of vegetation has been shown to result in realistic simulated vegetation dynamics in numerous studies using the offline LPJ-GUESS model (Smith et al., 2001;Hickler et al., 2012;Smith et al., 2014;Wårlind et al., 2014;Wu et al., 2015;Weber et al., 2009). Biophysical feedbacks have previously been studied in applications of RCA-GUESS to Europe and the Arctic (Wramneby et al., 2010;Smith et al., 2011;Zhang et al., 2014). A general description for the coupling between the vegetation dynamics component LPJ-GUESS and the physical component RCA is provided in the Appendix. A more detailed description is given by Smith et al. (2011).

2.2 Model setup, experiments and analysis approach

The simulations were applied over the African domain of the Coordinated Regional Climate Downscaling Experiment (CORDEX-Africa, Giorgi et al., 2009;Jones et al., 2011) on a horizontal grid with a resolution of 0.44° × 0.44°. The period studied was 1961 to 2100. Forcing (atmospheric fields and sea-surface temperature as lateral and lower boundary conditions) followed the historical and RCP8.5 simulations with the CanESM2 general circulation model (GCM) (Arora et al., 2011) in the Coupled Model Intercomparison Project Phase 5 (CMIP5, Taylor et al., 2012).

The vegetation sub-model LPJ-GUESS was set up with eight global PFTs which represent the major groups of natural vegetation across Africa, including the tropical and warm-temperate forests and C_3 and C_4 grass. The characteristics for the PFTs are based on the study by Morales et al. (2007). They are summarised in Table A1.

PFTs in the forest tile were simulated with 30 replicate patches. Average values of state variables across the replicate patches were used to determine biophysical parameters, i.e. forest fraction and leaf area index (LAI) for trees versus grasses, provided as forcing to the physical part of the model. For the open land tile with herbaceous species, C_3 and C_4 grass were simulated deterministically and aggregated to characterise open land vegetation. Fire disturbance in response to climate and simulated fuel load (Thonicke et al., 2001) was included.

Following the approach of Wramneby et al. (2010) and Smith et al. (2011), RCA-GUESS was initialized with a spin-up in two stages to achieve a quasi-steady state representative for mid-1900's conditions. After the spin-up, the model was run in coupled mode from 1961 onwards, with simulated dynamic meteorological conditions from the physical sub-model affecting vegetation phenology and structural dynamics, and biophysical land surface properties being adjusted to reflect the changes in vegetation, thereby affecting the physical climate dynamics. For comparison, a recent past experiment (RP, Table 1) with the same vegetation spin-up but then driven by the boundary condition from ECMWF re-analysis (ERA-Interim) project (Berrisford et al., 2009), was conducted for the period 1979-2011.

A simulation protocol was designed for inferring biophysical feedbacks of vegetation changes to the evolving 21st century climate. Three simulations were performed to investigate vegetation-climate feedbacks under future climate change (Table 1). The first simulation included the vegetation feedback (FB). It was run for 1961-2100 in coupled mode, allowing the effects of climate and atmospheric CO_2 concentration (the latter was taken directly from the RCP 8.5 data set) on vegetation state to feed back to the evolving climate. The second simulation was run without the vegetation feedback (NFB). It started with the state of FB simulation at 1991 and used a prescribed climatology of daily vegetation for 1961-1990 from the coupled simulation, but without allowing the simulated changes in vegetation in LPJ-GUESS to feed back to the simulated climate in RCA. To investigate the importance of the CO_2 physiological effects on vegetation changes under future climate change, we performed a third simulation (FB_CC), which was similar to FB, but starting from the state of FB simulation of 1991 and using historical atmospheric CO_2 forcing until 2005 and constant afterward for the vegetation sub-model.

In the analysis, we focus on the future period 2081-2100 and compare this with the present-day (1991-2010). The climate change signal is inferred from the difference between the future mean and the present-day mean in the NFB run. Vegetation feedbacks are calculated as the difference between the future means of the FB and NFB runs. These approaches were applied for the entire study, unless specified otherwise.

2.3 Methods to evaluate model performance

Simulated near-surface atmospheric temperature over open land, precipitation, and vegetation variable leaf area index (LAI) were compared against observations within the common available time period 1997-2010. Temperature and precipitation were compared with gridded observations from the CRU TS3.21 (Harris et al., 2014) dataset, focusing on the annual mean and seasonality. For precipitation we also employed the GPCP (Huffman et al., 2001, version 1.2 of One-Degree Daily product for 1996/10-2011/6) which uses satellite data

Earth Syst. Dynam. Discuss., doi:10.5194/esd-2015-88, 2016
Manuscript under review for journal Earth Syst. Dynam.
Published: 18 January 2016

to upscale rain gauge measurements and has been extensively used for African precipitation studies (e.g., Nikulin et al., 2012). For the LAI evaluation we used the GIMMS-AVHRR and MODIS-based LAI3g product (Zhu et al., 2013) which has been previously applied for the evaluation of vegetation dynamics in ESMs (e.g., Anav et al., 2013).

To identify biases propagating from the model physics per se and from the GCM-derived boundary forcing data, we compared the reanalysis-driven RP simulation against observation and against the GCM-driven (CanESM2) FB simulation for the same period.

3. Results

3.1 Model evaluation

To evaluate the model's performance for the present day, the simulated annual mean and seasonality of 2-meter air temperature, precipitation and LAI are compared against the observations (Fig. 1 and Fig. 2). The simulated annual mean temperature (Fig. 1a1) is generally higher in northern-hemisphere Africa than in the south. The model generally shows a cold bias in the order of 1°C for northern and southern savannah (Fig. 1a2), dominated by the boreal summer (Fig. 2a1,2a3). Warm biases occur over northern Africa up to around 3°C, as well as in central Africa (around 2°C) where the warm bias originates mainly from summer (Fig. 2a2).

The simulated precipitation is largest over western and central Africa up to 1600 mm year^{-1} within the simulated rainbelt between 25°N and 25°S, where the Atlantic moisture inflow (monsoon and equatorial westerlies) plays an important role (Fig. 1b1). Comparison with CRU reveals a considerable dry bias (-600 mm year^{-1}) for the central African rainforest area and a wet bias (+300 mm year^{-1}) for the northern savannah. A comparison of the FB

(CanESM2-driven) and the RP (ERA-Interim-driven) simulations (Fig. 1b3) indicates that apart from the uncertainty from RCM, the bias in simulated precipitation can be partly explained by the uncertainty from the boundary conditions. The simulated patterns and magnitude of precipitation for this area are similar to a previous study using an earlier version of RCA, RCA3.5, without dynamic vegetation (Nikulin et al., 2012). RCA3.5 was able to capture the main features of the seasonal mean rainfall distribution and its annual cycle, and the model biases were of similar magnitude to the differences between observational datasets (Nikulin et al., 2012).

The biases in simulated precipitation for the savannah regions and the central African rainforest area mirror the temperature biases: warm biases coincide with dry biases in central Africa, and cold biases coincide with wet biases in savannah regions. Apart from the model uncertainty, observation uncertainty may contribute to the biases, which can be seen when compared with GPCP (Fig. 2b1, 2b2): For the northern savannah, CRU tends to present lower precipitation than GPCP and the modelled throughout the year. For the central African rainforest area, precipitation from CRU is considerably higher in the mid-year dry season, but lower for the rest of the year with much more moderate monthly precipitation variability than in GPCP and the modelled. In general, the simulated precipitation presents a better consistency with GPCP than with CRU, although it is difficult to evaluate the uncertainties between these two observational datasets.

The simulated seasonality of LAI generally reflects the simulated seasonality of precipitation. A systematic overestimation is apparent for savannahs, and an underestimation for the central Africa rainforest area. These biases in LAI predominantly reflect the corresponding biases in precipitation (Fig. 2 b1-b3 and 2c1-c3). A stronger LAI bias in the savannah can be

Earth Syst. Dynam. Discuss., doi:10.5194/esd-2015-88, 2016
Manuscript under review for journal Earth Syst. Dynam.
Published: 18 January 2016

explained by the presence of grasses, which are more sensitive to precipitation changes in the model compared to trees.

With present-day forcing, the simulated climate and vegetation patterns and phenology are generally consistent with observed patterns. Some of the biases in the simulated climate are common to most RCMs (Nikulin et al., 2012) and they are apparent for some sub-regions and seasons in our model. However, we consider the performance adequate to capture the main details of the African climatology, which provides sufficient confidence for the subsequent analysis of regional vegetation-climate interactions under future climate change.

3.2 Future climate and vegetation change

In the simulation without vegetation feedbacks (NFB) under the RCP8.5 scenario and CanESM2 boundary conditions, most of the African continent is simulated to be 4-6°C warmer by the end of the 21st century (Fig. 3a). The subtropics exhibit a slightly stronger warming than the tropics, and land warming is slightly larger than warming of the surrounding ocean surface (note that the SSTs were prescribed from the GCM). These changes are fairly similar throughout the year, except in Northern Africa and the Sahara, where the temperature increase is particularly pronounced in the local dry season (Fig. A1e-h). Precipitation is projected to increase in most parts of the African monsoon area, western equatorial coastal area and the eastern African horn (Fig. A2e-h). A slight decrease is projected in the Congo basin and for the southern part of the continent (Fig. 3c). For areas with a precipitation increase, the increase is mainly confined to the local wet season. The precipitation decrease over central and southern Africa is apparent throughout the year (Fig. A2e-h).

Earth Syst. Dynam. Discuss., doi:10.5194/esd-2015-88, 2016
Manuscript under review for journal Earth Syst. Dynam.
Published: 18 January 2016

Vegetation feedbacks (FB) modify significantly the pattern and magnitude of simulated climate change. The effects are largest in low-latitude areas where the surface temperature increase is generally dampened (negative feedback), most notably in savannah areas and to a lesser extent in the equatorial rainforest area (Fig. 3b). The precipitation decrease is enhanced (positive feedback), most notably over rainforest (Fig. 3d).

With the effects of climate change and CO_2 fertilization, future vegetation growth depicts an enhancement not only of vegetation productivity in general, but also of tree cover in subtropical savannah areas (Fig. 4a), displacing grasses and resulting in an increase in tree LAI of 0.5-2.4 during the growing season (Fig. 4b). This increase in tree cover reflects a general rise in vegetation productivity driven by rising atmospheric CO_2 concentration on photosynthesis and water-use efficiency (Long, 1991;Hickler et al., 2008;Keenan et al., 2013). Results from the FB_CC experiment in which CO_2 fertilisation is disabled reveal that changes in climate drivers alone are simulated to have minor or opposing effects on tree productivity and LAI due to reduced water availability (Fig. A3), and that the changes above hence originate primarily from CO_2 fertilization.

Temperature feedbacks tend to be strong in the newly afforested areas (Fig. 3b, Fig. 4a). The cooling effects from vegetation feedbacks are strong (approximately -2°C) throughout the year, with the most pronounced cooling occurring in the local dry season (Fig. A1i-l), when the newly established forest (with larger root depth than grass) transpires water that is taken up from the deeper soil layer. Transpiration from present-day grass is constrained by the low moisture levels in the top soil layer. As a result, the evaporative cooling effect becomes stronger when forest replaces open land. In the central African rainforest area with increase of LAI by about 0.5-1, vegetation feedbacks on temperature are much smaller in the

Earth Syst. Dynam. Discuss., doi:10.5194/esd-2015-88, 2016
Manuscript under review for journal Earth Syst. Dynam.
Published: 18 January 2016

rainy season, but cause considerable cooling effect for the dry season.

Vegetation feedbacks on precipitation are also pronounced. For the Southern hemisphere savannah area, a slight increase in precipitation (approximately 10%, Fig. 3d) was simulated, which is caused by strengthened convective activity (which coincides with enhanced radiation and latent heat fluxes) in the rainy season (DFJ, Fig. A2). This can be considered as a local effect from forest expansion. However, changes in precipitation are not restricted only to the areas where forests expand (Fig. 3d, Fig. 4a), which is suggestive of remote effects for tropical precipitation. This is further investigated in the sections below.

3.3 Vegetation feedback effects on circulation and precipitation

Vegetation feedbacks on temperature in our simulations operate mainly via an increased surface area for evaporation and a stronger coupling to the atmosphere as tree cover, root depth and LAI increase relative to grasses, most notably in savannah areas, resulting in a shift of the evaporative fraction (ratio of latent heat flux to turbulent heat fluxes) and an increase in surface roughness length. Overall, the turbulent heat fluxes increase, which tends to cool the surface and the lower atmosphere. Similar behaviour was seen in southern Europe a feedback study with RCA-GUESS (Wramneby et al., 2010).

The variability of precipitation over Africa is greatly influenced by the moisture advection from the ocean to land. Studies have noted on the influence of Atlantic Walker circulation on central African precipitation, as well as the role of the west African monsoon (WAM) for the precipitation for western Africa (e.g. Nicholson and Grist, 2003;Nicholson and Dezfuli, 2013;Dezfuli and Nicholson, 2013). These circulation systems are associated with thermal contrasts between ocean and land, creating a pressure contrast that tends to promote the movement of moist surface air from the Atlantic over land. We examined the land-ocean thermal contrast (∇T) and geopotential contrast (∇ϕ) between the equatorial Atlantic and the near-coast African continent for three pressure levels between 850 hPa and 975 hPa, to investigate the circulation in the lower troposphere. We found that changes in ∇T and ∇ϕ are highly inter-annually anti-correlated for the rainy seasons MAM and SON (r=-0.82 and -0.64, respectively, Fig. 5; Fig. A4). The sensitivity of ∇ϕ to ∇T, depicted as the slope in Fig. 5, is generally maintained in the future, with a slight decrease in the sensitivity for DJF and a slight increase for MAM.

Under the NFB future simulation, ocean-land contrast becomes larger (the absolute value of ∇T increases by about 0.5-1°C, Table A2) as land temperature increases more than the ocean surface temperature (Fig. A1), due to differential changes in features of the surface and lower atmosphere, such as changes in land-ocean contrasts in boundary layer lapse rate (Joshi et al., 2008) and changes in Bowen ratio over land (Sutton et al., 2007). As a result, except for SON, ∇ϕ is generally simulated to increase in the course of the simulation (Fig. A4), with the largest shift occurring in MAM (11.96 $m^2 s^{-2}$ by the end of 21st century, Table A2). For SON, ∇T increases but ∇ϕ does not, suggesting that the trend of ∇ϕ under climate change is associated with the GCM-derived boundary conditions, despite the strong regional coupling with ∇T in terms of variability (Fig. A4).

In contrast, the increase in the ∇T is dampened considerably when incorporating interactive vegetation. The resulting reduction in ∇T offsets ∇ϕ uniformly and statistically significantly for all seasons, generally counteracting the climate change effect on ∇ϕ (Fig. 5, Table A2).

3.4 Effects on Walker circulation and low-latitude precipitation

Earth Syst. Dynam. Discuss., doi:10.5194/esd-2015-88, 2016
Manuscript under review for journal Earth Syst. Dynam.
Published: 18 January 2016

The low-level equatorial westerlies are important to the central African rainfall. They are associated with the lower branch of the Walker cell located near the western equatorial coast of Africa, and they transfer moisture from the adjacent Atlantic to the eastern equatorial coast and the Congo basin (e.g. Schefuß et al., 2005;Nicholson and Grist, 2003). These westerlies occur from March to October, being best developed in JJA. They shift northward with the excursion of the Inter Tropical Convergence Zone (ITCZ) and under the strong influence of the South Atlantic high pressure cell (Nicholson and Grist, 2003). This pattern is simulated by RCA-GUESS for the present-day climate (Fig. 6). Via this circulation system, moisture can reach far over the African landmass at around 28°E, upwell and integrate into the mid-level African Easterly Jet (AEJ) (Camberlin et al., 2001;Nicholson and Grist, 2003). RCA-GUESS reproduces this pattern with a realistic magnitude (Fig. 6, Fig. 7, Fig. 8, Fig. 9) when compared with previous studies based on reanalysis data (Camberlin et al., 2001;Nicholson and Grist, 2003).

In the NFB future simulation, equatorial westerlies are strengthened throughout the year both over ocean (Fig. 6) and over land (Fig. 7). Changes in wind speed (Δu) can be explained by changes in the low-level pressure contrast between land and ocean (sect. 3.3), where strengthened $\nabla\phi$ leads to enhanced u, especially for MAM when the zonal pressure contrast prevails (Table A2). Atmospheric specific humidity in the lower troposphere near the equator also increases by around 10%-20% for MAM and SON, extending from the ocean to inland along the equator (Fig. 8cd; Fig. 9cd). Meanwhile, changes in future rainfall are apparent along the equator, with increases over the equatorial coastal or inland areas (Fig. A2), concurrent with stronger moisture inflow to land in the low-level troposphere (Fig. 8cd; Fig. 9cd).

Earth Syst. Dynam. Discuss., doi:10.5194/esd-2015-88, 2016
Manuscript under review for journal Earth Syst. Dynam.
Published: 18 January 2016

Vegetation feedbacks are simulated to weaken the climate change enhancement of the Walker circulation, resulting in a weakening of the equatorial westerlies and counteracting the effects of climate change alone (Fig. 6i-l and Fig. 7i-l; Fig. 8ef and Fig. 9ef). These changes correspond well to changes in low-level ocean-land geopotential contrast $\Delta\nabla\phi$ with the biggest impact for MAM and SON (Table A2). The weakened Walker circulation is also represented as suppressed vertical uplifting motions over central Africa (Fig. 8f and Fig. 9f). Atmospheric specific humidity at 850 hPa is reduced by approximately 7% due to vegetation feedbacks which are comparable to the contribution of climate change (Fig. 8ef vs. Fig. 8cd; Fig. 9ef vs. Fig. 9cd).

Analysis of the moisture flux convergence also confirms the impacts of a weakened Walker circulation (Fig. 10) on the hydrological cycle caused by vegetation feedback. Moisture fluxes for most parts of the African continent diverge toward the ocean near the equatorial regions. This divergence is similar for both MAM and SON but the effect is slightly stronger for SON, which also corresponds to reduced humidity for these areas (Fig. 8e-f; Fig. 9e-f).

The changes in precipitation show a distinct spatial and temporal pattern with changes in the rainbelt area (defined as 2mm day^{-1} contour with 10-days smoothing, Fig. 11). Under future conditions, the rainbelt, which follows the ITCZ excursion, shifts around 3° northward during JAS (Fig. 11a). As a result, rainfall intensity increases from May to October, with the most pronounced increase by more than 30% relative to present-day levels of around 2 mm day^{-1} on the margins of the rainbelt. The rainy season becomes longer for Sahel (+9 days) as well as for central Africa (+1 day). The location of the rainbelt for the rest of the year remains unchanged, but there is a pronounced increase in rainfall intensity for southern African rainy season (about 10%) and a decrease (about -10%) for the central African rainy

Earth Syst. Dynam. Discuss., doi:10.5194/esd-2015-88, 2016
Manuscript under review for journal Earth Syst. Dynam.
Published: 18 January 2016

seasons.

On top of the non-feedback climate change effect, vegetation feedbacks tend to cause a slight contraction of the rainbelt around the equator, and they impose a primarily counteractive effect on rainfall intensity compared to the climate change alone simulation (NFB). For central Africa, the considerable decrease in rainfall intensity in the dry season leads to a slight equatorward shrinking of the rainbelt (approximately 2°) and a shorter rainy season (on average 10 days, represented as a 4-day postponed onset and a 6-day earlier end). For southern Africa, strengthened convective precipitation results in a longer rainy season by on average 6 days. There is no pronounced effect for the Sahel regions except for some sparse changes over time and in some areas. To investigate the effects on ITCZ location, we analysed the position of the intertropical front (ITF) with a meridional wind criterion (Sultan and Janicot, 2003) by examining the location of maximum vertical uplifting wind speed at 850 hPa over Sahel in July and over southern Africa in January. However, we did not find pronounced effects for ITF (not shown) suggesting that changes in the rainbelt location for central Africa are mainly caused by changes in precipitation intensity rather than by changes in meridional circulation.

4. Discussion

4.1 Related tenets of Regional Earth System Modelling

Previous studies on land-climate interactions for Africa were carried out either over some African sub-region (e.g. Wang and Alo, 2012;Yu et al., 2015), or at a relatively coarse resolution within the implementation of GCMs (e.g. Kucharski et al., 2013), or without considering feedback effects from natural vegetation dynamics and only investigating anthropogenic impacts such as deforestation or afforestation (Lawrence and Vandecar, 2015). In this study, we investigated the coupled dynamics of climate and vegetation patterns over Africa under a future climate change scenario, applying a regional-scale ESM. The development of regional-scale coupling, including vegetation dynamics in a coherent way, enables the quantification of vegetation-change-induced feedbacks in climate simulations (Rummukainen, 2010;Smith et al., 2011;Giorgi, 1995;Zhang et al., 2014;Wramneby et al., 2010). In this way, it is able to isolate the regional biophysical feedbacks, which are usually not easy to disentangle in a global application in which the effects of changes in carbon-cycle and large-scale circulation tend to combine with the biophysical effects.

In comparison with global ESMs, the added value from the regional ESMs lies in the enhanced resolution obtained in a regional setup as presented in this study, allowing for a more detailed representation of small-scale surface features such as topography, land use, vegetation change, and consequently possible related feedbacks, and also enhancing the model's ability to capture climatic variability and extreme climatic events (Rummukainen, 2010). In addition, improvements in the representation of local processes (e.g. those that determine surface temperature) may result in improved larger scale features (e.g. sea level pressure) (Feser, 2006;Diffenbaugh et al., 2005). As seen also in a previous evaluation study for the atmosphere-only version of RCA for Europe, a reduced bias in surface air temperature results in a better representation of interannual variability of mean sea level pressure and circulation patterns, and improves the simulation of precipitation (Kjellström et al., 2005).

4.2 Vegetation dynamics over Africa for present and future

Earth Syst. Dynam. Discuss., doi:10.5194/esd-2015-88, 2016
Manuscript under review for journal Earth Syst. Dynam.
Published: 18 January 2016

Vegetation dynamics are critically important in modulating the evolution of the 21st century climate in our study. Land use and grazing (Lindeskog et al., 2013;Bondeau et al., 2007;Sankaran et al., 2005), which were not included in our study, represent additional drivers of land surface changes. The historical vegetation state is also relevant for future simulations, due to legacy effects lasting decades or even centuries (Wang et al., 2004;Moncrieff et al., 2014). Apart from the biases in climate (model) forcing, biases in simulated vegetation may come from the absence of consideration of these aspects and result in over- or under-estimation of the vegetation state. Nevertheless, the vegetation-feedback effects associated with the vegetation sub-model are still likely to be captured here, as vegetation dynamics in terms of forest cover changes and interannual and inter-seasonal variability of vegetation productivity are more important than the absolute vegetation state when considering vegetation feedbacks. Previous studies in the offline vegetation model LPJ-GUESS suggests that the vegetation dynamics for savannah and tropical forest vegetation are robust (Weber et al., 2009;Ahlström et al., 2015), providing additional confidence for the examination of the vegetation-climate interaction in our study.

Under future climate change, the vegetation response to environmental changes will differ. As revealed by previous experimental (Kgope et al., 2010) and modelling (Sitch et al., 2008;Moncrieff et al., 2014) studies, vegetation may be expected to become less sensitive to climate conditions when the atmospheric CO_2 concentration increases. This is because CO_2 fertilization of photosynthesis and enhanced water use efficiency linked to a reduction of stomatal conductance, which causes a shift towards higher woody-plant dominance, resulting in densification of tree and shrub cover relative to grasses in savannahs, or replacement of savannah with forest. Shrub encroachment and woody thickening has been observed in water-limited areas including Sahel in recent decades, coinciding with rising CO_2 concentrations (e.g. Liu et al., 2015). In our results, the simulated vegetation dynamics are consistent with these trends, presenting a similar trajectory of vegetation changes (not shown), and a similar vegetation pattern (Fig. A3) as in previous modelling studies (e.g., Sitch et al., 2008;Moncrieff et al., 2014).

4.3 Vegetation feedbacks and land-ocean temperature contrasts

The land-ocean contrast is an important driver of continental precipitation, as it determines the transport of moisture from ocean to land (e.g. Lambert et al., 2011;Fasullo, 2010;Giannini et al., 2005;Boer, 2011;Giannini et al., 2003). The recent change in Sahel rainfall is a good example of linking moisture transport to land-ocean contrast, where changes in SSTs over adjacent tropical oceans around Africa are key to the fragile balance that defines the regional circulation system (Rowell, 2001;Giannini et al., 2003;Camberlin et al., 2001). Land-surface feedback is found to modify the interannual to interdecadal climate variability in this region by vegetation-induced albedo or evapotranspiration effects (Charney, 1975;Zeng et al., 1999;Wang et al., 2004). In our study, the SSTs were prescribed from CanESM2, therefore the altered land-ocean thermal contrast between simulations with and without feedback originated solely from the changes in land surface temperature induced by vegetation dynamics. Although this represents a land-forced mechanism in contrast to an ocean-forced one in other studies (e.g. Giannini et al., 2003;Tokinaga et al., 2012), we assume that the mechanisms are similar given the similarity in the magnitude of simulated circulation changes. Wind speed and land-ocean temperature contrast change approximately by 0.2 m s^{-1} and 0.2°C, respectively, between FB and NFB in our study (Fig. 5 and Table A2); these are comparable to the changes simulated in other studies for the Sahel (approximately 0.2-0.5 m s^{-1} per 0.2°C (Giannini et al., 2005)) and for the Pacific Oceans (approximately 0.3 m s^{-1} per 0.3°C (Tokinaga et al., 2012)). However, the relative importance of such changes may differ for local climate systems: the lower branch of the Walker cell over the eastern tropical Atlantic Ocean, which we have focused on in this study, may be in a fragile balance and is more vulnerable to changes in thermal contrasts (equatorial westerlies slowed down by approximately 0.2 m s^{-1} from less than 2 m s^{-1} of the present-day wind speed in rainy seasons, Table A2) compared to the stronger monsoonal circulation for Sahel and the Walker cell over the equatorial Pacific Ocean (> 5 m per second wind speed in their peak months, Young, 1999). Our results indicate that even a small disturbance of the eastern Tropical Atlantic circulation cell may produce profound impacts (larger relative reduction in precipitation compared with the studies by Giannini et al. (2005) *and* Tokinaga et al. (2012)). Moreover, we assume that a study with a dynamic ocean component would result in a similar outcome, as the ocean heat capacity is relatively large and variation in land-ocean thermal contrast can be greatly buffered by ocean heat uptake (Lambert and Chiang, 2007).

5. Conclusion and outlook

In this study we investigated the potential role of vegetation-mediated biophysical feedbacks on climate change projections for Africa in the 21st century. In current savannah regions, enhanced forest growth results in a strong evaporative cooling effect. We also identify alterations in the large-scale circulation induced by savannah vegetation change, resulting in remote effects and modulation of tropical rainfall patterns in Africa. Our results emphasize the importance of accounting for vegetation-atmosphere interactions in regional climate projections for tropical and sub-tropical Africa and stress the necessity to consider

Earth Syst. Dynam. Discuss., doi:10.5194/esd-2015-88, 2016
Manuscript under review for journal Earth Syst. Dynam.
Published: 18 January 2016

vegetation feedbacks for more reliable estimates of regional future climate change projections.

Future work can include detailed studies on the role of vegetation feedbacks in the regional climate projections with respect to shorter-term dynamics such as climate variability and extreme events, which may have crucial implications for land surface processes such as wildfire. On the other hand, regional and global biogeochemical feedbacks on future climate change may be triggered by regional biophysical feedbacks, which can impose important influences to regional climatic trend, variability and seasonality in conjunction with future greenhouse forcing. Such changes may impose important influences on the African carbon balance, especially for the semi-arid ecosystem like savannahs whose carbon balance is strongly associated with changes in climatic conditions (Ahlström et al., 2015). Further examination of vegetation feedback effect in regional ESMs may have its distinct values especially when regional processes are concerned. Future work should also include the ongoing development of ESMs including the improvement of the system's ability to represent land surface properties by incorporating important land surface processes such as changes in land use (e.g. forest clearing/grazing) and land management (e.g. irrigation), for use in versatile land-atmospheric interaction studies.

Appendix A: Description for the coupling between RCA and LPJ-GUESS

In RCA-GUESS, the LSS in RCA is coupled with LPJ-GUESS, which feeds back vegetation properties to RCA. RCA provides net downward shortwave radiation, air temperature, precipitation to LPJ-GUESS. In return, LPJ-GUESS provides daily updated LAI and the annually updated tile sizes (determined from the simulated maximum growing season LAI summed across tree and herbaceous PFTs in the previous year (Smith et al., 2011)). In the forest tile in RCA, vegetation cover in this tile is estimated as the foliar projective cover (FPC) using Beer's law:

$$\mathrm{A}_{tree} = 1.0 - \exp(-0.5 \cdot LAI_{tree}), \tag{1}$$

where LAI_{tree} is the aggregated LAI of woody species, simulated by LPJ-GUESS in its forest tile in which vegetation is assumed to comprise trees and understory herbaceous vegetation. The natural vegetated faction of the open land tile was calculated similarly:

$$\mathrm{A}_{grass} = 1.0 - \exp(-0.5 \cdot LAI_{grass}), \tag{2}$$

where LAI_{grass} is the summed LAI of the simulated herbaceous PFTs from the herbaceous tile of LPJ-GUESS in which only herbaceous vegetation is allowed to grow. The relative covers of the forest and open land tiles affect surface albedo, which is a weighted average of prescribed albedo constants for forest, open land and bare soil and controls the absorption of surface incoming solar radiation, and therefore influences surface energy balance and temperature.

The turbulent heat fluxes are influenced by the properties of each tile, such as surface roughness and surface resistance, which partly depend on vegetation properties provided by LPJ-GUESS. The vegetation surface resistance controls vegetation transpiration and bare soil evaporation for latent heat flux calculation. It scales with LAI and varies between the

Earth Syst. Dynam. Discuss., doi:10.5194/esd-2015-88, 2016
Manuscript under review for journal Earth Syst. Dynam.
Published: 18 January 2016

different types of vegetation and affected by the incoming photosynthetically active radiation, soil-water stress, vapour pressure deficit, air temperature and soil temperature. The aerodynamic resistance controls both latent heat flux and sensible heat flux and is influenced by surface roughness length distinguished from open land and forest. The total heat fluxes and heat transfer determine the time evolution of the surface temperature and thus the thermodynamics in the lower boundary layer. More details about the LSS are given in Samuelsson et al. (2006), and the description of its coupling to the vegetation sub-model is provided by Smith et al. (2011).

Table A1. Characteristics of the plant functional types (PFTs) used in the vegetation sub-model LPJ-GUESS.

Characteristics	NE	BE	TrBE	TrBR	TBS	IBS	C3G	C4G
Leaf phenology[a]	E	E	E	D	D	D	R	R
Drought tolerance	low	low	low	low	low	low	very low	very low
Shade tolerance	high	high	high	low	high	low	low	Low
Optimal temperature range for photosynthesis (°C)	10-25	15-35	25-30	25-30	15-25	10-25	10-30	20-45
Min T_c for survival (°C)[b]	-	1.7	15.5	15.5	-18	-	-	15.5

Notes: NE, needleleaved evergreen tree; BE, broadleaved evergreen tree; TrBE, tropical broadleaved evergreen tree; TrBR, tropical broadleaved raingreen tree; TBS, shade-tolerant broadleaved summergreen tree; IBS, shade-intolerant broadleaved summergreen tree; C3G, C3 grass or herb; C4G, C4 grass or herb;
[a]E, evergreen; D, deciduous; R, raingreen.
[b]T_c = mean temperature (°C) of coldest month of year.

Earth Syst. Dynam. Discuss., doi:10.5194/esd-2015-88, 2016
Manuscript under review for journal Earth Syst. Dynam.
Published: 18 January 2016

571 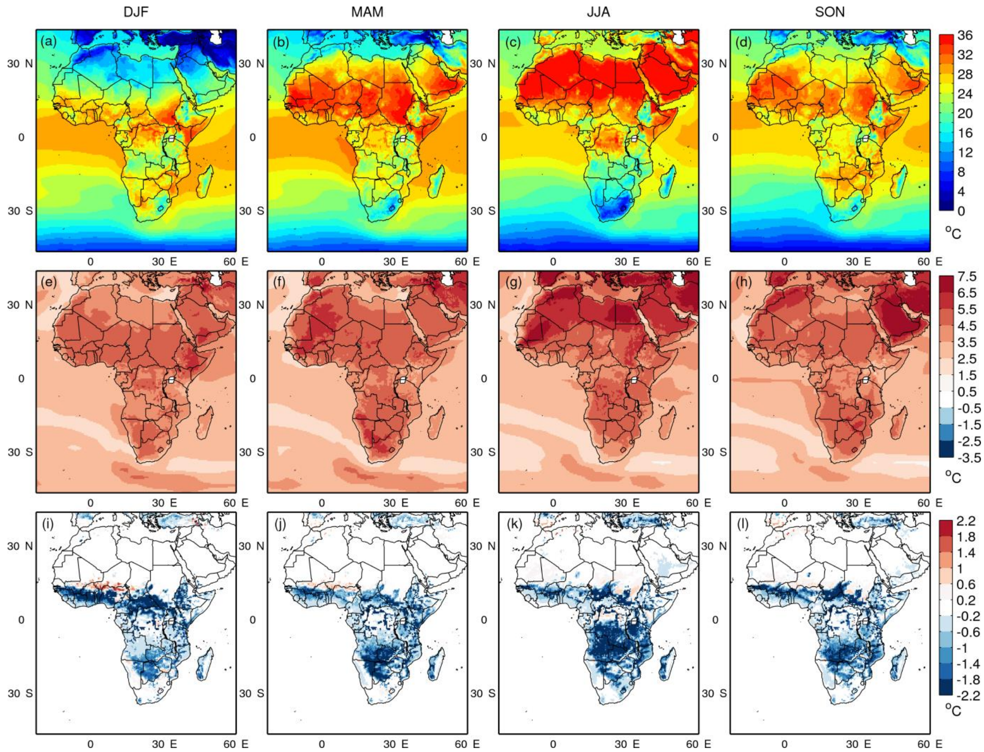

572 Fig. A1. Seasonal surface temperature: 1st panel, for present day; 2nd panel, changes in future in the NFB
573 experiment; 3rd panel, changes from vegetation feedback, represented as FB minus NFB for future.

574

Earth Syst. Dynam. Discuss., doi:10.5194/esd-2015-88, 2016
Manuscript under review for journal Earth Syst. Dynam.
Published: 18 January 2016

Earth System Dynamics
Discussions
Open Access

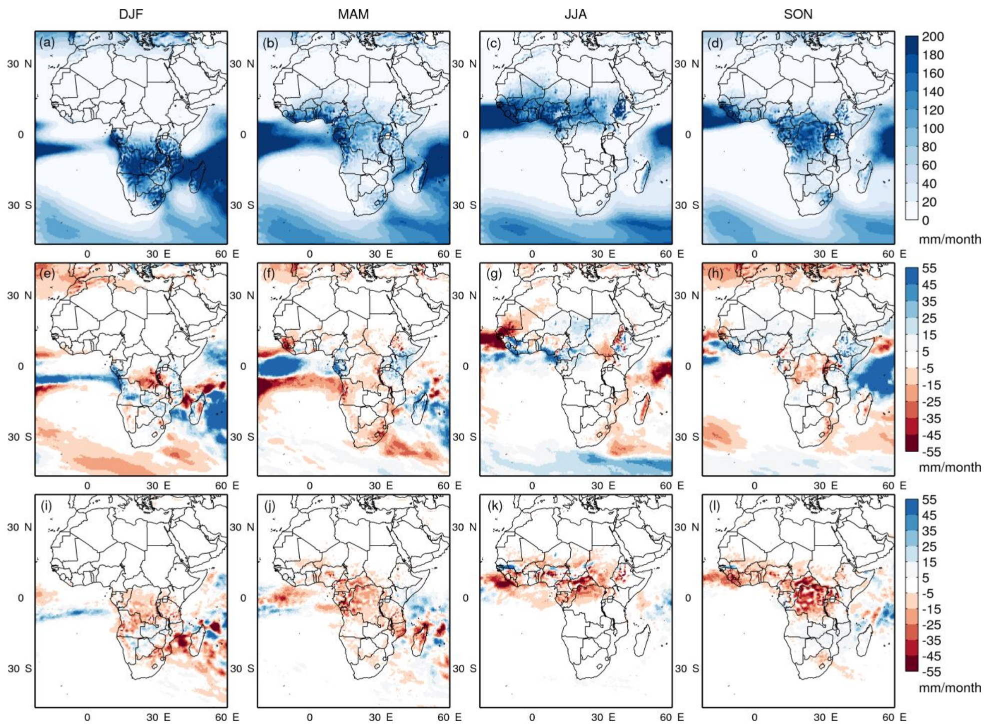

Fig. A2. Similar to Fig. A1, but for precipitation.

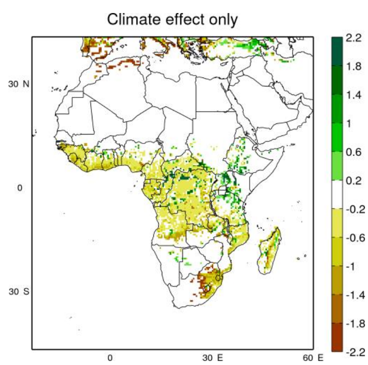

Fig. A3. Changes in forest tile LAI from the period 1991-2010 to the period 2081-2100 in FB_CC experiment.

Earth Syst. Dynam. Discuss., doi:10.5194/esd-2015-88, 2016
Manuscript under review for journal Earth Syst. Dynam.
Published: 18 January 2016

Earth System Dynamics
Discussions
Open Access

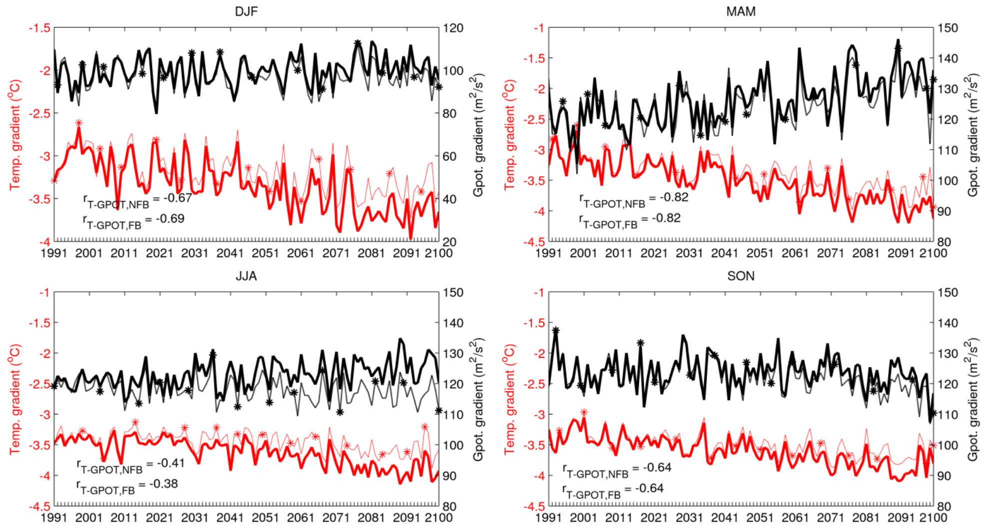

Fig. A4. Annual changes in atmospheric ocean-land temperature contrast (∇T) and geopotential contrast (∇ϕ) in time series for four seasons, represented by the mean contrast at the three pressure levels 850, 925 and 975 hPa (ocean minus land) within the domain 15°N-15°S, 24°W-20°E (see the inset in the panel for JJA in Fig. 5). Correlation coefficient (r) between atmospheric temperature contrast (∇T) and geopotential contrast (∇ϕ) are computed based on the de-trended annual time-series values for both FB (thick lines) and NFB (thin lines with asterisks) simulations. Changes between FB and NFB are significant at 95% confidence level for the whole time period. Note the different y-axis for DJF.

Table A2. Atmospheric temperature contrast, geopotential contrast and westerlies wind speed for the present-day state and contributions from climate change (CC subscript) and vegetation feedbacks (FB subscript), standard deviation is in parenthesis.

	DJF	MAM	JJA	SON
$\nabla T_{present\text{-}day}$ (°C) [a]	-3.06 (0.30)	-3.15 (0.34)	-3.47 (0.22)	-3.37 (0.24)
$\Delta\nabla T_{CC}$ (°C) [a]	-0.59*	-0.73*	-0.45*	-0.47*
$\Delta\nabla T_{FB}$ (°C) [a]	0.29*	0.23*	0.31*	0.22*
$\nabla\phi_{present\text{-}day}$ ($m^2 s^{-2}$) [a]	98.14 (5.92)	120.86 (7.03)	120.94 (3.83)	124.08 (4.58)
$\Delta\nabla\phi_{CC}$ ($m^2 s^{-2}$) [a]	3.94	11.96*	4.73*	-3.32
$\Delta\nabla\phi_{FB}$ ($m^2 s^{-2}$) [a]	-4.93*	-3.86*	-8.96*	-3.92*
$u_{zonal,present\text{-}day}$ ($m s^{-1}$) [b]	0.01 (0.27)	1.47 (0.32)	0.87 (0.37)	1.22 (0.31)
$\Delta u_{zonal,CC}$ ($m s^{-1}$) [b]	0.35*	0.32*	0.68*	0.17*
$\Delta u_{zonal,FB}$ ($m s^{-1}$) [b]	-0.00	-0.21*	-0.28*	-0.16*

Note: [a]: Calculations are same as Fig. 5.
[b]: u_{zonal} is the averaged zonal wind speed for the pressure levels 850, 925 and 975 hPa between 3.5°N-6.5°N and 0-10°E; The positive represents westerly and the negative represents easterly.
*: Changes are significant at 95% confidence level using Mann-Whitney U-test (Hollander and Wolfe, 1999).

Acknowledgement

This study is a contribution to the strategic research areas Modelling the Regional and Global Earth System (MERGE) and Biodiversity and Ecosystem Services in a Changing Climate (BECC). MCW would like to thanks Paul Miller for his helpful discussion and comments on this work. This work was performed at the National Supercomputer Centre (NSC) in Linköping, Sweden.

Earth Syst. Dynam. Discuss., doi:10.5194/esd-2015-88, 2016
Manuscript under review for journal Earth Syst. Dynam.
Published: 18 January 2016

Earth System Dynamics Discussions
Open Access

Reference

Ahlström, A., Raupach, M. R., Schurgers, G., Smith, B., Arneth, A., Jung, M., Reichstein, M., Canadell, J. G., Friedlingstein, P., and Jain, A. K.: The dominant role of semi-arid ecosystems in the trend and variability of the land CO2 sink, Science, 348, 895-899, 2015.

Anav, A., Friedlingstein, P., Kidston, M., Bopp, L., Ciais, P., Cox, P., Jones, C., Jung, M., Myneni, R., and Zhu, Z.: Evaluating the Land and Ocean Components of the Global Carbon Cycle in the CMIP5 Earth System Models, Journal of Climate, 26, 6801-6843, 10.1175/jcli-d-12-00417.1, 2013.

Arora, V., Scinocca, J., Boer, G., Christian, J., Denman, K., Flato, G., Kharin, V., Lee, W., and Merryfield, W.: Carbon emission limits required to satisfy future representative concentration pathways of greenhouse gases, Geophysical Research Letters, 38, 2011.

Avissar, R., and Werth, D.: Global hydroclimatological teleconnections resulting from tropical deforestation, Journal of Hydrometeorology, 6, 134-145, 2005.

Bell, J. P., Tompkins, A. M., Bouka - Biona, C., and Seidou Sanda, I.: A process - based investigation into the impact of the Congo Basin deforestation on surface climate, Journal of Geophysical Research: Atmospheres, 2015.

Berrisford, P., Dee, D., Fielding, K., Fuentes, M., Kallberg, P., Kobayashi, S., and Uppala, S.: The ERA-Interim Archive, 2009.

Boer, G.: The ratio of land to ocean temperature change under global warming, Climate dynamics, 37, 2253-2270, 2011.

Bonan, G. B.: Forests and climate change: forcings, feedbacks, and the climate benefits of forests, science, 320, 1444-1449, 2008.

Bondeau, A., Smith, P. C., Zaehle, S., Schaphoff, S., Lucht, W., Cramer, W., Gerten, D., LOTZE - CAMPEN, H., Müller, C., and Reichstein, M.: Modelling the role of agriculture for the 20th century global terrestrial carbon balance, Global Change Biology, 13, 679-706, 2007.

Brovkin, V., Claussen, M., Driesschaert, E., Fichefet, T., Kicklighter, D., Loutre, M.-F., Matthews, H., Ramankutty, N., Schaeffer, M., and Sokolov, A.: Biogeophysical effects of historical land cover changes simulated by six Earth system models of intermediate complexity, Climate Dynamics, 26, 587-600, 2006.

Camberlin, P., Janicot, S., and Poccard, I.: Seasonality and atmospheric dynamics of the teleconnection between African rainfall and tropical sea - surface temperature: Atlantic vs. ENSO, International Journal of Climatology, 21, 973-1005, 2001.

Earth Syst. Dynam. Discuss., doi:10.5194/esd-2015-88, 2016
Manuscript under review for journal Earth Syst. Dynam.
Published: 18 January 2016

Charney, J. G.: Dynamics of deserts and drought in the Sahel, Quarterly Journal of the Royal Meteorological Society, 101, 193-202, 1975.

Dezfuli, A. K., and Nicholson, S. E.: The relationship of rainfall variability in western equatorial Africa to the tropical oceans and atmospheric circulation. Part II: The boreal autumn, Journal of Climate, 26, 66-84, 2013.

Diffenbaugh, N. S., Pal, J. S., Trapp, R. J., and Giorgi, F.: Fine-scale processes regulate the response of extreme events to global climate change, Proceedings of the National Academy of Sciences of the United States of America, 102, 15774-15778, 10.1073/pnas.0506042102, 2005.

Doherty, R. M., Sitch, S., Smith, B., Lewis, S. L., and Thornton, P. K.: Implications of future climate and atmospheric CO2 content for regional biogeochemistry, biogeography and ecosystem services across East Africa, Global Change Biology, 16, 617-640, 2010.

Döscher, R., Wyser, K., Meier, H. M., Qian, M., and Redler, R.: Quantifying Arctic contributions to climate predictability in a regional coupled ocean-ice-atmosphere model, Climate Dynamics, 34, 1157-1176, 2010.

Eklundh, L., and Olsson, L.: Vegetation index trends for the African Sahel 1982–1999, Geophysical Research Letters, 30, 2003.

Eltahir, E. A.: Role of vegetation in sustaining large-scale atmospheric circulations in the tropics, JOURNAL OF GEOPHYSICAL RESEARCH-ALL SERIES-, 101, 4255-4268, 1996.

Fasullo, J. T.: Robust Land-Ocean Contrasts in Energy and Water Cycle Feedbacks*, Journal of Climate, 23, 4677-4693, 2010.

Feser, F.: Enhanced detectability of added value in limited-area model results separated into different spatial scales, Monthly weather review, 134, 2180-2190, 2006.

Giannini, A., Saravanan, R., and Chang, P.: Oceanic forcing of Sahel rainfall on interannual to interdecadal time scales, Science, 302, 1027-1030, 2003.

Giannini, A., Saravanan, R., and Chang, P.: Dynamics of the boreal summer African monsoon in the NSIPP1 atmospheric model, Climate Dynamics, 25, 517-535, 2005.

Giorgi, F.: Perspectives for regional earth system modeling, Global and Planetary Change, 10, 23-42, 1995.

Giorgi, F., Jones, C., and Asrar, G. R.: Addressing climate information needs at the regional level: the CORDEX framework, World Meteorological Organization (WMO) Bulletin, 58, 175, 2009.

Harris, I., Jones, P. D., Osborn, T. J., and Lister, D. H.: Updated high-resolution grids of monthly climatic observations – the CRU TS3.10 Dataset, International Journal of Climatology, 34, 623-642, 10.1002/joc.3711, 2014.

Herrmann, S. M., Anyamba, A., and Tucker, C. J.: Recent trends in vegetation dynamics in the African Sahel and their relationship to climate, Global

Environmental Change, 15, 394-404, http://dx.doi.org/10.1016/j.gloenvcha.2005.08.004, 2005.
Hickler, T., Eklundh, L., Seaquist, J. W., Smith, B., Ardö, J., Olsson, L., Sykes, M. T., and Sjöström, M.: Precipitation controls Sahel greening trend, Geophysical Research Letters, 32, 2005.
Hickler, T., Smith, B., Prentice, I. C., Mjofors, K., Miller, P., Arneth, A., and Sykes, M. T.: CO(2) fertilization in temperate FACE experiments not representative of boreal and tropical forests, Global Change Biology, 14, 1531-1542, 10.1111/j.1365-2486.2008.01598.x, 2008.
Hickler, T., Vohland, K., Feehan, J., Miller, P. A., Smith, B., Costa, L., Giesecke, T., Fronzek, S., Carter, T. R., and Cramer, W.: Projecting the future distribution of European potential natural vegetation zones with a generalized, tree species - based dynamic vegetation model, Global Ecology and Biogeography, 21, 50-63, 2012.
Hollander, M., and Wolfe, D. A.: in: Nonparametric Statistical Methods, 2nd ed., John Wiley & Sons, New York 35-140, 1999.
Huffman, G. J., Adler, R. F., Morrissey, M. M., Bolvin, D. T., Curtis, S., Joyce, R., McGavock, B., and Susskind, J.: Global precipitation at one-degree daily resolution from multisatellite observations, Journal of Hydrometeorology, 2, 36-50, 2001.
Jamali, S., Seaquist, J., Eklundh, L., and Ardö, J.: Automated mapping of vegetation trends with polynomials using NDVI imagery over the Sahel, Remote Sensing of Environment, 141, 79-89, http://dx.doi.org/10.1016/j.rse.2013.10.019, 2014.
Jones, C., Giorgi, F., and Asrar, G.: The Coordinated Regional Downscaling Experiment: CORDEX–an international downscaling link to CMIP5, Clivar Exchanges, 16, 34-40, 2011.
Joshi, M. M., Gregory, J. M., Webb, M. J., Sexton, D. M., and Johns, T. C.: Mechanisms for the land/sea warming contrast exhibited by simulations of climate change, Climate Dynamics, 30, 455-465, 2008.
Keenan, T. F., Hollinger, D. Y., Bohrer, G., Dragoni, D., Munger, J. W., Schmid, H. P., and Richardson, A. D.: Increase in forest water-use efficiency as atmospheric carbon dioxide concentrations rise, Nature, 499, 324-327, 2013.
Kgope, B. S., Bond, W. J., and Midgley, G. F.: Growth responses of African savanna trees implicate atmospheric [CO2] as a driver of past and current changes in savanna tree cover, Austral Ecology, 35, 451-463, 2010.
Kjellström, E., Bärring, L., Gollvik, S., Hansson, U., Jones, C., Samuelsson, P., Rummukainen, M., Ullerstig, A., Willén, U., and Wyser, K.: A 140-year simulation of European climate with the new version of the Rossby Centre regional atmospheric climate model (RCA3), 2005.

Earth Syst. Dynam. Discuss., doi:10.5194/esd-2015-88, 2016
Manuscript under review for journal Earth Syst. Dynam.
Published: 18 January 2016

Kjellström, E., Nikulin, G., Hansson, U., Strandberg, G., and Ullerstig, A.: 21st century changes in the European climate: uncertainties derived from an ensemble of regional climate model simulations, Tellus A, 63, 24-40, 2011.

Kucharski, F., Zeng, N., and Kalnay, E.: A further assessment of vegetation feedback on decadal Sahel rainfall variability, Climate dynamics, 40, 1453-1466, 2013.

Lambert, F. H., and Chiang, J. C.: Control of land - ocean temperature contrast by ocean heat uptake, Geophysical research letters, 34, 2007.

Lambert, F. H., Webb, M. J., and Joshi, M. M.: The relationship between land-ocean surface temperature contrast and radiative forcing, Journal of Climate, 24, 3239-3256, 2011.

Lawrence, D., and Vandecar, K.: Effects of tropical deforestation on climate and agriculture, Nature Climate Change, 5, 27-36, 2015.

Lindeskog, M., Arneth, A., Bondeau, A., Waha, K., Seaquist, J., Olin, S., and Smith, B.: Implications of accounting for land use in simulations of ecosystem carbon cycling in Africa, Earth System Dynamics, 4, 385-407, 2013.

Liu, Y. Y., van Dijk, A. I. J. M., de Jeu, R. A. M., Canadell, J. G., McCabe, M. F., Evans, J. P., and Wang, G.: Recent reversal in loss of global terrestrial biomass, Nature Clim. Change, 5, 470-474, 10.1038/nclimate2581

http://www.nature.com/nclimate/journal/v5/n5/abs/nclimate2581.html#supplementary-information, 2015.

Long, S.: Modification of the response of photosynthetic productivity to rising temperature by atmospheric CO2 concentrations: has its importance been underestimated?, Plant, Cell & Environment, 14, 729-739, 1991.

Moncrieff, G. R., Scheiter, S., Bond, W. J., and Higgins, S. I.: Increasing atmospheric CO2 overrides the historical legacy of multiple stable biome states in Africa, New Phytologist, 201, 908-915, 2014.

Morales, P., Hickler, T., Rowell, D. P., Smith, B., and Sykes, M. T.: Changes in European ecosystem productivity and carbon balance driven by regional climate model output, Global Change Biology, 13, 108-122, 2007.

Moss, R. H., Edmonds, J. A., Hibbard, K. A., Manning, M. R., Rose, S. K., Van Vuuren, D. P., Carter, T. R., Emori, S., Kainuma, M., and Kram, T.: The next generation of scenarios for climate change research and assessment, Nature, 463, 747-756, 2010.

Nicholson, S. E., and Grist, J. P.: The seasonal evolution of the atmospheric circulation over West Africa and equatorial Africa, Journal of Climate, 16, 1013-1030, 2003.

Nicholson, S. E., and Dezfuli, A. K.: The relationship of rainfall variability in western equatorial Africa to the tropical oceans and atmospheric circulation. Part I: The boreal spring, Journal of Climate, 26, 45-65, 2013.

Nikulin, G., Jones, C., Giorgi, F., Asrar, G., Büchner, M., Cerezo-Mota, R., Christensen, O. B., Déqué, M., Fernandez, J., Hänsler, A., van Meijgaard, E., Samuelsson, P., Sylla, M. B., and Sushama, L.: Precipitation Climatology in an Ensemble of CORDEX-Africa Regional Climate Simulations, Journal of Climate, 25, 6057-6078, 10.1175/JCLI-D-11-00375.1, 2012.

Nogherotto, R., Coppola, E., Giorgi, F., and Mariotti, L.: Impact of Congo Basin deforestation on the African monsoon, Atmospheric Science Letters, 14, 45-51, 2013.

Olsson, L., Eklundh, L., and Ardö, J.: A recent greening of the Sahel—trends, patterns and potential causes, Journal of Arid Environments, 63, 556-566, 2005.

Rowell, D. P.: Teleconnections between the tropical Pacific and the Sahel, Quarterly Journal of the Royal Meteorological Society, 127, 1683-1706, 2001.

Rummukainen, M.: State-of-the-art with regional climate models, Wiley Interdisciplinary Reviews: Climate Change, 1, 82-96, 10.1002/wcc.8, 2010.

Samuelsson, P., Gollvik, S., and Ullerstig, A.: The land-surface scheme of the Rossby Centre regional atmospheric climate model (RCA3), SMHI, 2006.

Samuelsson, P., Jones, C. G., Willén, U., Ullerstig, A., Gollvik, S., Hansson, U., Jansson, C., Kjellström, E., Nikulin, G., and Wyser, K.: The Rossby Centre Regional Climate model RCA3: model description and performance, Tellus A, 63, 4-23, 2011.

Sankaran, M., Hanan, N. P., Scholes, R. J., Ratnam, J., Augustine, D. J., Cade, B. S., Gignoux, J., Higgins, S. I., Le Roux, X., and Ludwig, F.: Determinants of woody cover in African savannas, Nature, 438, 846-849, 2005.

Schefuß, E., Schouten, S., and Schneider, R. R.: Climatic controls on central African hydrology during the past 20,000 years, Nature, 437, 1003-1006, 2005.

Sitch, S., Huntingford, C., Gedney, N., Levy, P. E., Lomas, M., Piao, S. L., Betts, R., Ciais, P., Cox, P., Friedlingstein, P., Jones, C. D., Prentice, I. C., and Woodward, F. I.: Evaluation of the terrestrial carbon cycle, future plant geography and climate-carbon cycle feedbacks using five Dynamic Global Vegetation Models (DGVMs), Global Change Biology, 14, 2015-2039, 10.1111/j.1365-2486.2008.01626.x, 2008.

Smith, B., Prentice, I. C., and Sykes, M. T.: Representation of vegetation dynamics in the modelling of terrestrial ecosystems: comparing two contrasting approaches within European climate space, Global Ecology and Biogeography, 10, 621-637, 10.1046/j.1466-822X.2001.t01-1-00256.x, 2001.

Smith, B., Samuelsson, P., Wramneby, A., and Rummukainen, M.: A model of the coupled dynamics of climate, vegetation and terrestrial ecosystem

Earth Syst. Dynam. Discuss., doi:10.5194/esd-2015-88, 2016
Manuscript under review for journal Earth Syst. Dynam.
Published: 18 January 2016

biogeochemistry for regional applications, Tellus A, 63, 87-106, 10.1111/j.1600-0870.2010.00477.x, 2011.

Smith, B., Warlind, D., Arneth, A., Hickler, T., Leadley, P., Siltberg, J., and Zaehle, S.: Implications of incorporating N cycling and N limitations on primary production in an individual-based dynamic vegetation model, Biogeosciences, 11, 2027-2054, 2014.

Sörensson, A. A., and Menéndez, C. G.: Summer soil–precipitation coupling in South America, Tellus A, 63, 56-68, 2011.

Sultan, B., and Janicot, S.: The West African monsoon dynamics. Part II: The "preonset" and "onset" of the summer monsoon, Journal of climate, 16, 3407-3427, 2003.

Sutton, R. T., Dong, B., and Gregory, J. M.: Land/sea warming ratio in response to climate change: IPCC AR4 model results and comparison with observations, Geophysical Research Letters, 34, n/a-n/a, 10.1029/2006GL028164, 2007.

Taylor, K. E., Stouffer, R. J., and Meehl, G. A.: An overview of CMIP5 and the experiment design, Bulletin of the American Meteorological Society, 93, 485-498, 2012.

Thonicke, K., Venevsky, S., Sitch, S., and Cramer, W.: The role of fire disturbance for global vegetation dynamics: coupling fire into a Dynamic Global Vegetation Model, Global Ecology and Biogeography, 10, 661-677, 10.1046/j.1466-822X.2001.00175.x, 2001.

Tokinaga, H., Xie, S.-P., Deser, C., Kosaka, Y., and Okumura, Y. M.: Slowdown of the Walker circulation driven by tropical Indo-Pacific warming, Nature, 491, 439-443, 2012.

Wang, G., and Eltahir, E.: Ecosystem dynamics and the Sahel drought, Geophys Res Lett, 27, 795 - 798, 2000.

Wang, G., Eltahir, E., Foley, J., Pollard, D., and Levis, S.: Decadal variability of rainfall in the Sahel: results from the coupled GENESIS-IBIS atmosphere-biosphere model, Climate Dynamics, 22, 625-637, 2004.

Wang, G., and Alo, C. A.: Changes in precipitation seasonality in West Africa predicted by RegCM3 and the impact of dynamic vegetation feedback, International Journal of Geophysics, 2012, 2012.

Wårlind, D., Smith, B., Hickler, T., and Arneth, A.: Nitrogen feedbacks increase future terrestrial ecosystem carbon uptake in an individual-based dynamic vegetation model, Biogeosciences, 11, 6131-6146, 10.5194/bg-11-6131-2014, 2014.

Weber, U., Jung, M., Reichstein, M., Beer, C., Braakhekke, M., Lehsten, V., Ghent, D., Kaduk, J., Viovy, N., and Ciais, P.: The interannual variability of Africa's ecosystem productivity: a multi-model analysis, Biogeosciences, 6, 285-295, 2009.

Earth Syst. Dynam. Discuss., doi:10.5194/esd-2015-88, 2016
Manuscript under review for journal Earth Syst. Dynam.
Published: 18 January 2016

Wramneby, A., Smith, B., and Samuelsson, P.: Hot spots of vegetation-climate feedbacks under future greenhouse forcing in Europe, J. Geophys. Res., 115, D21119, 10.1029/2010jd014307, 2010.

Wu, M., Knorr, W., Thonicke, K., Schurgers, G., Camia, A., and Arneth, A.: Sensitivity of burned area in Europe to climate change, atmospheric CO2 levels and demography: A comparison of two fire - vegetation models, Journal of Geophysical Research: Biogeosciences, 10.1002/2015JG003036, 2015.

Xue, Y., and Shukla, J.: The influence of land surface properties on Sahel climate. Part 1: desertification, Journal of climate, 6, 2232-2245, 1993.

Xue, Y., and Shukla, J.: The Influence of Land Surface Properties on Sahel Climate. Part Π: Afforestation, 1996.

Young, I.: Seasonal variability of the global ocean wind and wave climate, International Journal of Climatology, 19, 931-950, 1999.

Yu, M., Wang, G., and Pal, J. S.: Effects of vegetation feedback on future climate change over West Africa, Climate Dynamics, 1-20, 2015.

Zeng, N., Neelin, J. D., Lau, K.-M., and Tucker, C. J.: Enhancement of interdecadal climate variability in the Sahel by vegetation interaction, Science, 286, 1537-1540, 1999.

Zhang, W., Jansson, C., Miller, P., Smith, B., and Samuelsson, P.: Biogeophysical feedbacks enhance the Arctic terrestrial carbon sink in regional Earth system dynamics, Biogeosciences, 11, 5503-5519, 2014.

Zhou, L., Tian, Y., Myneni, R. B., Ciais, P., Saatchi, S., Liu, Y. Y., Piao, S., Chen, H., Vermote, E. F., Song, C., and Hwang, T.: Widespread decline of Congo rainforest greenness in the past decade, Nature, 509, 86-90, 10.1038/nature13265, 2014.

Zhu, Z., Bi, J., Pan, Y., Ganguly, S., Anav, A., Xu, L., Samanta, A., Piao, S., Nemani, R. R., and Myneni, R. B.: Global data sets of vegetation leaf area index (LAI) 3g and Fraction of Photosynthetically Active Radiation (FPAR) 3g derived from Global Inventory Modeling and Mapping Studies (GIMMS) Normalized Difference Vegetation Index (NDVI3g) for the period 1981 to 2011, Remote Sensing, 5, 927-948, 2013.

Earth Syst. Dynam. Discuss., doi:10.5194/esd-2015-88, 2016
Manuscript under review for journal Earth Syst. Dynam.
Published: 18 January 2016

Earth System Dynamics
Discussions
Open Access

Figures and Tables

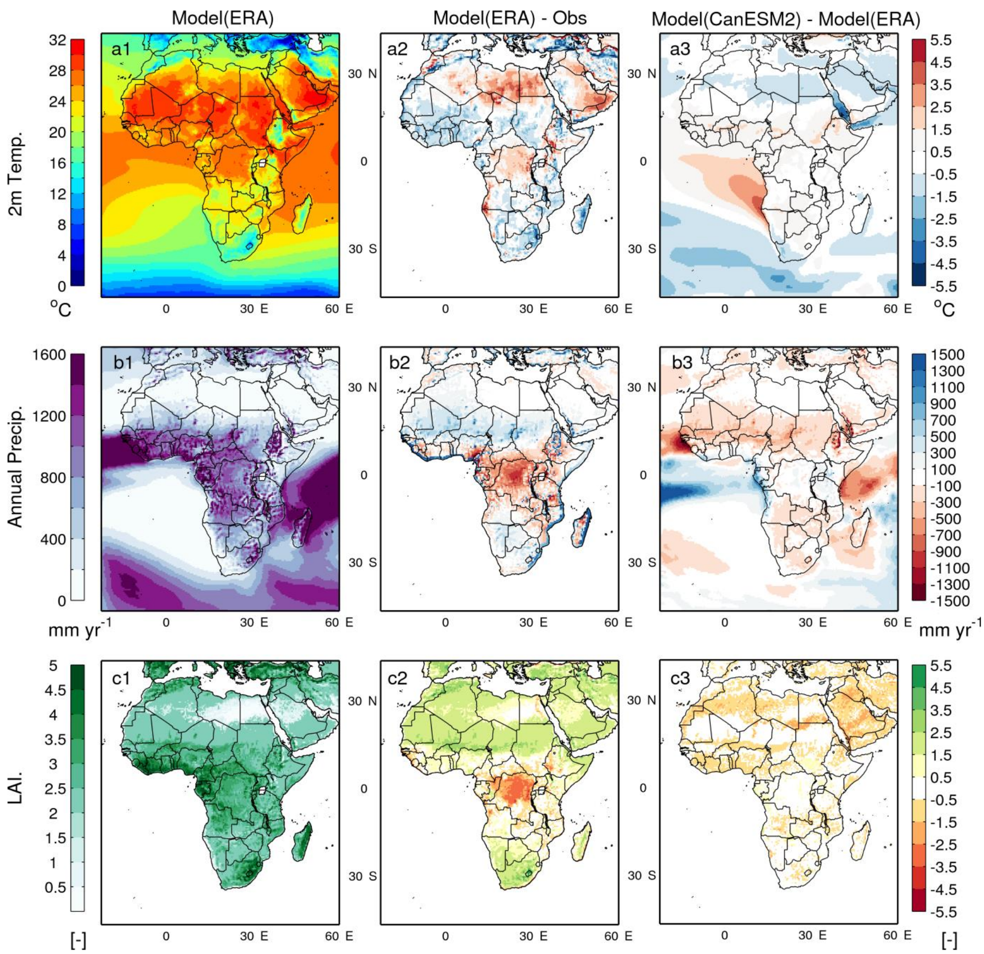

Fig. 1. Comparison between simulated and observed (a) annual mean near-surface air temperature, (b) annual precipitation and (c) annual maximum LAI for the period 1997-2010. Variables from the RP experiment (a1-c1) are compared with observations (a2-c2) and with those from the FB experiment (a3-c3), using RP minus observation and FB minus RP. For the comparison with observations (a2-c2), we used CRU temperature (a2) and precipitation (b2), as well as LAI3g (Zhu et al., 2013)(c2).

Earth Syst. Dynam. Discuss., doi:10.5194/esd-2015-88, 2016
Manuscript under review for journal Earth Syst. Dynam.
Published: 18 January 2016

901 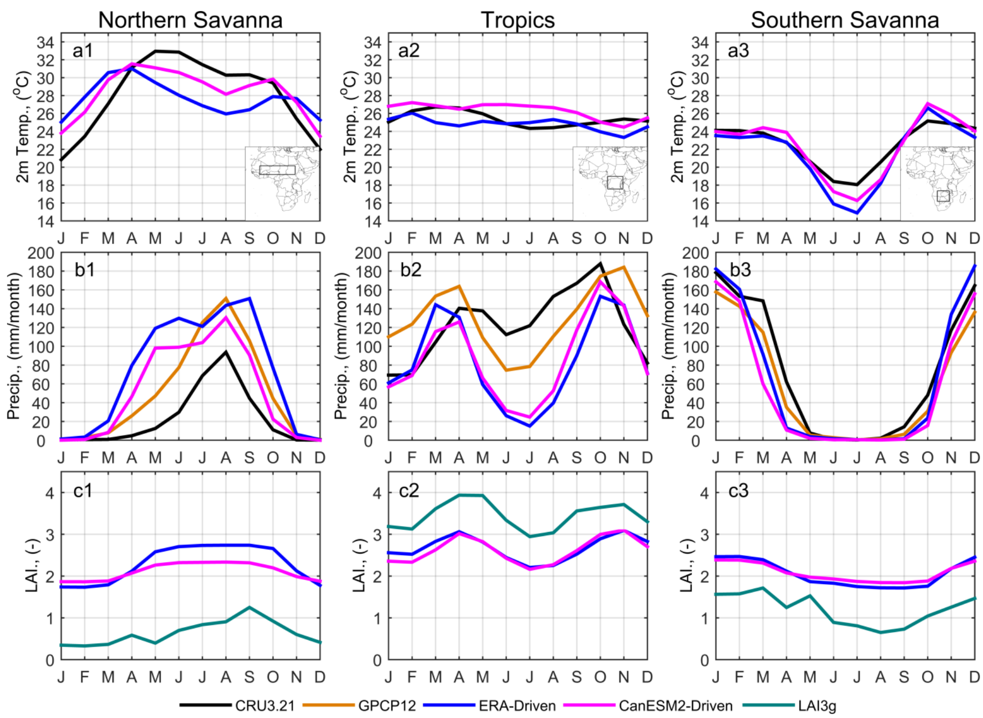

902 Fig. 2. Simulated seasonal cycle and observations for northern savannah (inset in a1), central Africa (inset
903 in a2) and southern savannah (inset in a3) for the period 1997-2010. 2m temperature (a1-a3) and precipitation
904 (b1-b3) are as Fig. 1. For LAI (c1-c3) monthly mean tile-weighted simulated LAI over the averaging period are
905 used to compare with the observation.

Earth Syst. Dynam. Discuss., doi:10.5194/esd-2015-88, 2016
Manuscript under review for journal Earth Syst. Dynam.
Published: 18 January 2016

Earth System Dynamics
Discussions
Open Access

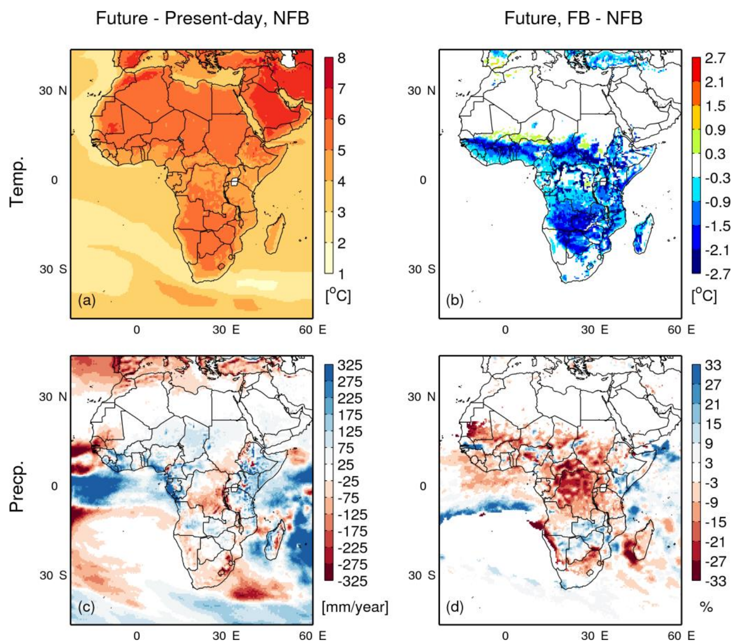

Fig. 3. Changes in surface temperature and precipitation due to climate change and vegetation feedback. The calculation of climate change signal and vegetation feedbacks, present-day and future periods are defined in Sect. 2.2. For (d), the percentage is calculated as the difference between FB and NFB (vegetation feedback) divided by the present-day level and multiplied by 100. Grid points with annual mean precipitation <20 mm year^{-1} are skipped.

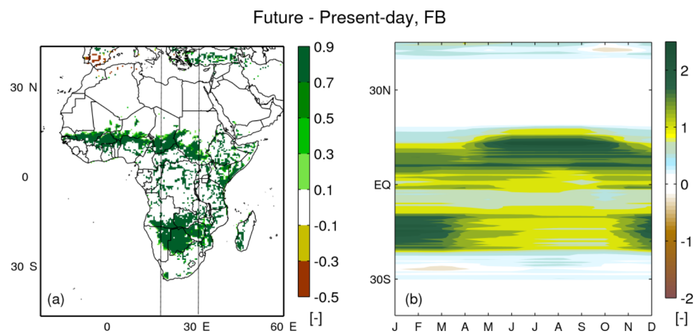

Fig. 4. (a) Change in forest fraction and (b) seasonal change in zonal mean forest LAI in the longitude band between 18°E and 30°E (lines in a), calculated as future minus present-day in FB experiment. Present-day and future periods are defined in Sect. 2.2.

Earth Syst. Dynam. Discuss., doi:10.5194/esd-2015-88, 2016
Manuscript under review for journal Earth Syst. Dynam.
Published: 18 January 2016

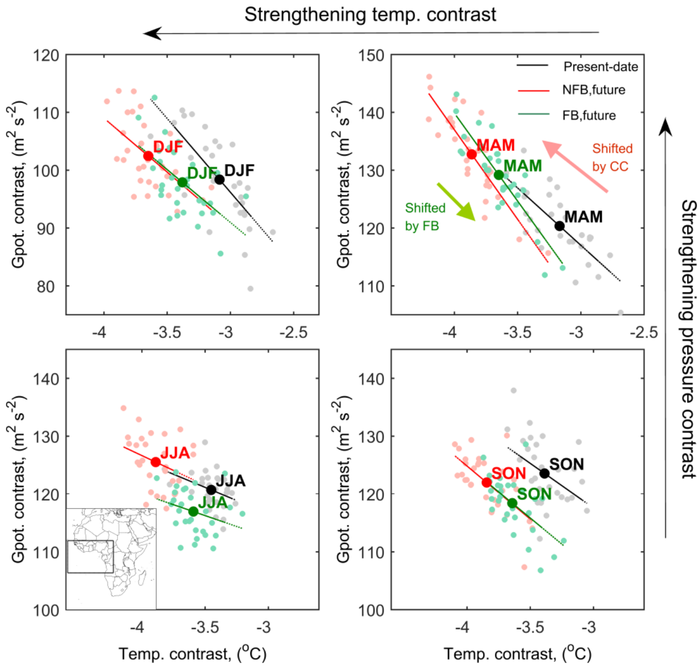

Fig. 5. Changes in atmospheric ocean-land temperature contrast (∇T) and geopotential contrast ($\nabla \phi$), represented by the mean contrast at the three pressure levels 850, 925 and 975 hPa (ocean minus land) within the domain 15°N-15°S, 24°W-20°E (see the inset in the panel for JJA), for the NFB and FB simulation in the present-day and the future period (as defined in Sect. 2.2). Each scatter point represents the relation between $\nabla \phi$ and ∇T for the correspondent season of one year, and the slopes represent its sensitivity during the selected periods.

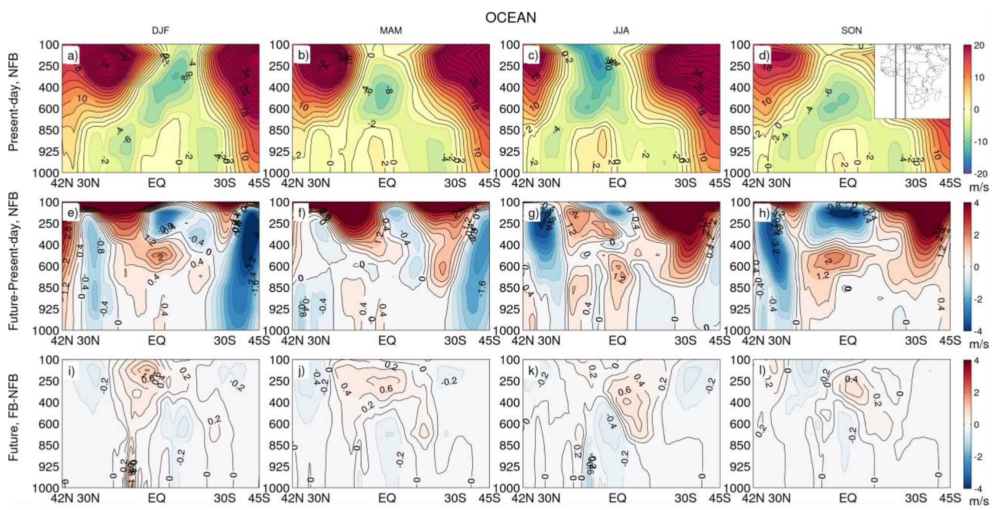

Fig. 6. Seasonal mean zonal wind speed in a cross section over adjacent Atlantic ocean (0-10°E, see the inset in d), for present-day (1st row), changes in future (future minus present-day, 2nd row) and the differences between FB and NFB runs in future (FB minus NFB, 3rd row). Unit is m s^{-1}, positive values represent

Earth Syst. Dynam. Discuss., doi:10.5194/esd-2015-88, 2016
Manuscript under review for journal Earth Syst. Dynam.
Published: 18 January 2016

Earth System Dynamics
Discussions

westerlies and negative values represent easterlies. Present-day and future periods are defined in Sect. 2.2 Contour intervals from top row to bottom row are 2m s^{-1}, 0.4m s^{-1} and 0.2m s^{-1}, respectively.

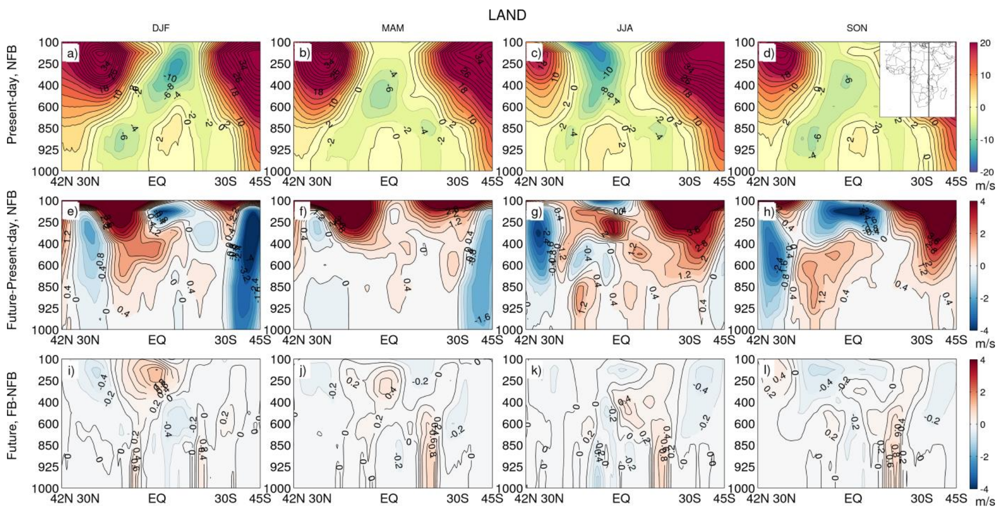

Fig. 7. As Fig. 6 but for longitudinal band over land (10°E-30°E, see the inset in d).

Earth Syst. Dynam. Discuss., doi:10.5194/esd-2015-88, 2016
Manuscript under review for journal Earth Syst. Dynam.
Published: 18 January 2016

Earth System Dynamics
Discussions

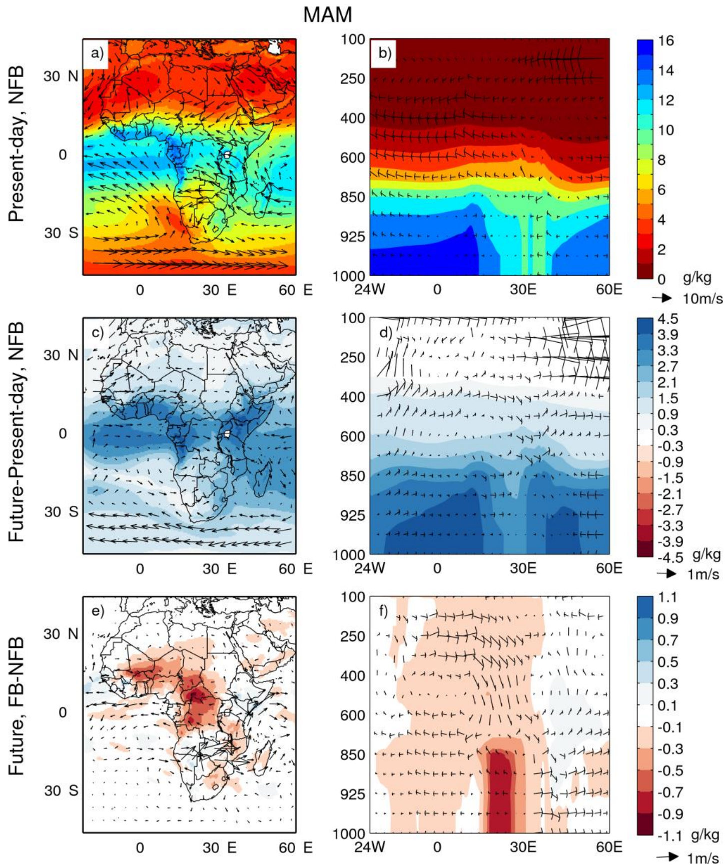

Fig. 8. Atmospheric circulation (arrows, m s^{-1}) and specific humidity (colour contours, g kg^{-1}) at 850 hPa pressure level for MAM, displayed as (a, c, e) for the entire domain, and (b, d, f) as a cross section for a latitude band between 2.5°S and 2.5°N, for present day (top), climate change impacts (middle) and the vegetation feedback (bottom). Definitions for calculation period, climate change signal and vegetation feedbacks are given in Sect. 2.2.

Earth Syst. Dynam. Discuss., doi:10.5194/esd-2015-88, 2016
Manuscript under review for journal Earth Syst. Dynam.
Published: 18 January 2016

Earth System Dynamics
Discussions
Open Access

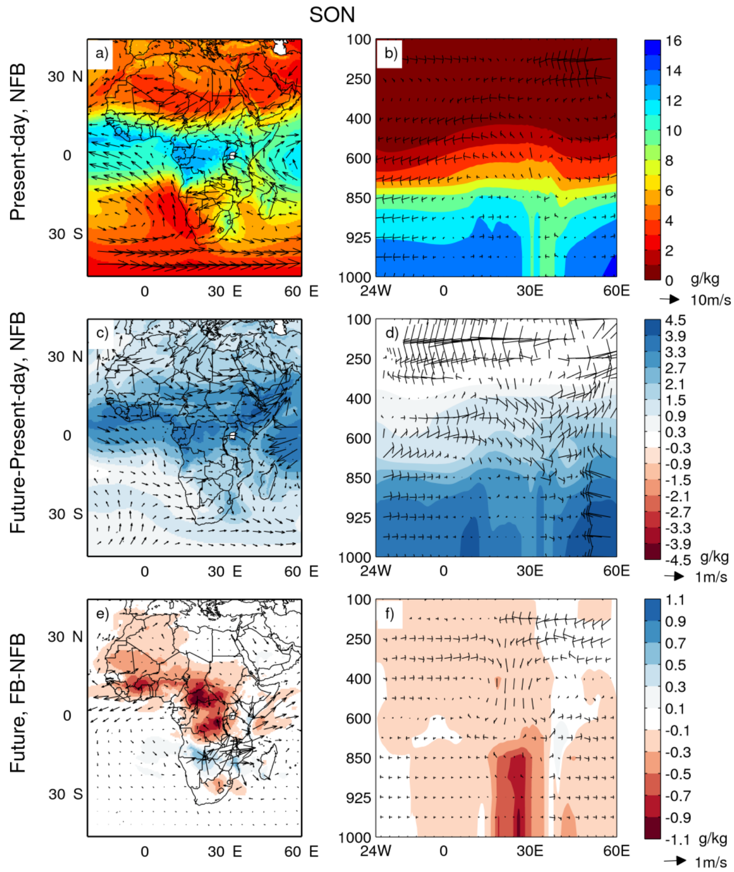

Fig. 9. As Fig. 8 but for SON.

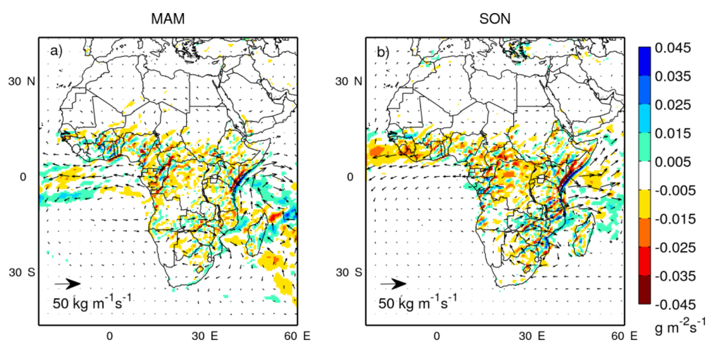

Fig. 10. Changes in vertically integrated moisture flux (arrows, kg m^{-1}s^{-1}) and moisture flux convergence (colour contours, g m^{-2}s^{-1}) caused by vegetation feedback, averaged over the future period (as defined in Sect. 2.2) for (a) MAM and (b) SON.

Earth Syst. Dynam. Discuss., doi:10.5194/esd-2015-88, 2016
Manuscript under review for journal Earth Syst. Dynam.
Published: 18 January 2016

Earth System Dynamics
Discussions
Open Access

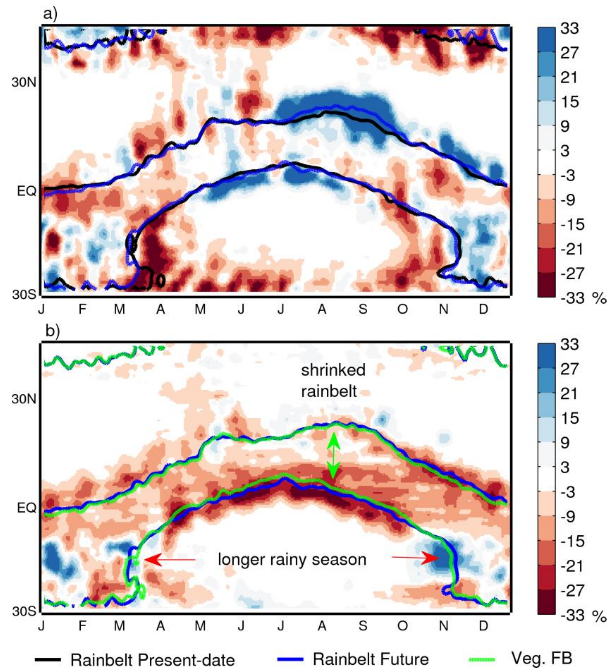

Fig. 11. Daily changes in precipitation averaged over the longitude band 18°E-30°E, represented as relative changes in daily precipitation intensity (shading, %) and rainbelt location (contour) due to (a) climate change and (b) vegetation feedback for future. The rainbelt location is defined as 2mm day^{-1} contour. 10-day running mean is applied for daily values.

Table 1. Experimental design for the investigation of the vegetation-climate feedbacks in this study.

Runs	Vegetation Feedbacks	Radiative forcing[a]	CO_2 forcing[b] for vegetation sub-model	Simulated period	Boundary condition
RP	Dynamic	Historical	Historical	1979-2011	ERA-Interim
FB	Dynamic	Transient under RCP8.5	Transient under RCP8.5	1961-2100	CanESM2
NFB	Prescribed vegetation simulated from 1961 to 1990	Transient under RCP8.5	Transient under RCP8.5	1991-2100	CanESM2
FB_CC	Dynamic	Transient under RCP8.5	Historical until 2005 and constant afterward	1991-2100	CanESM2

Notes: a, using equivalent atmospheric CO_2 concentration; b, using actual atmospheric CO_2 concentration.